Article:
Boretto, Gabriella, Zanchetta, Giovanni, Ciulli, Lorenzo et al. (8 more authors) (2017) The loess deposits of Buca Dei Corvi section (Central Italy): Revisited. Catena. pp. 225-237. ISSN: 0341-8162

https://doi.org/10.1016/j.catena.2017.01.001

THE "LOESS" DEPOSITS OF BUCA DEI CORVI SECTION (CENTRAL ITALY) REVISITED

Gabriella Boretto.[1,4],Giovanni Zanchetta[1,2,3*], Lorenzo Ciulli[1**], Monica Bini[1], Anthony E. Fallick[5], Marco Lezzerini[1], Andre C. Colonese[6], Irene Zembo[7***], Luca Trombino[7], Eleonora Regattieri[8], Giovanni Sarti[1]

[1]Dipartimento di Scienze della Terra, Via S. Maria 53, 56126, Pisa, Italy (**present adress ciulli.lorenzo@alice.it)
[2]IGG-CNR, Via Moruzzi, 1 56100 Pisa, Italy
[3]INGV Sez. di Pisa, Via della Faggiola, 32, 56100 Pisa
[4]CONICET, INGEA UNLP, calle 64 no 3, 1900 La Plata, Argentina
[5]Scottish Universities Environmental Research Centre, East Kilbride G75 0QF, Scotland (UK).
[6]Department of Archaeology, BioArCh, University of York, Wentworth Way, York YO10 5DD England (UK).
[7]University of Milan Earth Sciences Department "A. Desio" Via Mangiagalli, 34 20133-I Milano, Italy, (***present address zemboirene@gmail.com)
[8]IGAG-CNR, Via Salaria km 29,300 00015 Monterotondo Rome, Italy
*Corresponding author: E-mail address: zanchetta@dst.unipi.it

Abstract

Loess deposits have been described in the past for the upper section of Buca Dei Corvi succession (Central Italy). In this paper the deposits were re-analyzed to clarify the depositional environment and to attempt a paleoclimate reconstruction. Two radiocarbon dates on pedogenic carbonate constrain the ages to the Late Glacial, and are consistent with previous OSL dating of the top of the succession. The non-marine mollusc assemblage shows typical character of cold and dry climatic conditions, testified by strong oligotypical composition. Mineralogy and geochemistry of the sediments indicate the abundant presence of exotic quartz mineral which can be explained only by wind transport. Probably, wind transport was also responsible of deposition of carbonate which then dissolved and re-precipitated producing pedogenic concretions. Stable isotopes ($^{13}C/^{12}C$ and $^{18}O/^{16}O$ ratios) of the concretions are consistent with a climate drier than present conditions, with an environment characterized by sparse vegetation.

Keywords: non-marine molluscs, pedogenic carbonate, stable isotopes, Late Glacial, Italy

1.Introduction

In the review of loess deposits throughout Italy, Cremaschi (1990) did not report any finding south-west of the Apennine chain. More recently, the possibility of the occurrence of phases of aeolian dust aggradation during cold periods in more southerly positions than previously reported has been re-assessed (e.g. Giraudi et al., 2013). Specifically for Tuscany, Sarti et al. (2005), reported evidence of loess deposition within the succession cropping out at the Gulf of Baratti (Fig. 1). In this paper we discuss the presence of loess deposits in the Buca dei Corvi section (Fig. 1), one of the most important Late Quaternary sections of the Tyrrhenian coast of Central Italy, and report new stratigraphic, chronological, paleontological and geochemical data. The "Buca dei Corvi" section (literally "the Hole of the Ravens" 43°24'47'' N 10°24'12'') is one of the best studied and most completely exposed Late Quaternary geological successions on the Tyrrhenian coast north of Rome, and contains a discontinuous record of the Upper Pleistocene sea level oscillations. In particular, the basal level is a rich marine fossil-bearing site, containing the so-called "warm guests" mollusc (Blanc, 1953, Ottman, 1954; Nisi et al., 2003), and it was one of the sections anchored with aminostratigraphy in the classic work of Hearty et al. (1986) on the Mediterranean raised beaches. On the basis of this work the basal fossiliferous coastal deposit was correlated with the Marine Isotope Stage 5e (MIS5e). Subsequently, Mauz (1999) obtained new age measurements, using the optically stimulated luminescence technique (OSL), for the basal layer (>108 ka) then 94±34 at intermediate depth, and finally 9.7± ka for the upper part of the section. As a result, the Buca dei Corvi is one of the few relatively well-dated coastal successions of Late Quaternary of the Tyrrhenian coast of Italy (e.g. Hearty et al., 1986, Mauz, 1999). Interestingly Ottman (1954) reported the presence of fine-grained "loess" deposits in the top part of the succession in the road cut of the Via Aurelia close to Castiglioncello village (Fig. 1). The presence of these deposits was not further investigated and they represent the target of this contribution.

2.Geological and morphological setting

The coastal area can be grossly divided in two main morphological units corresponding to Terrazzo I and Terrazzo II of Federici and Mazzanti (1995). The "Terrazzo I" corresponds to a polycyclic marine-continental terrace with the base related to marine transgression culminating in the high stand of MIS5e (Federici and Mazzanti, 1995; Zanchetta et al., 2006). The "Terrazzo II", which locally is uplifted to ca. 125 m a.s.l., is again a polycyclic terrace, probably originating at the MIS11

(Zanchetta et al., 2006). The Buca dei Corvi section is located at a narrow coastal inlet at the northern sector of the "Terrazzo I", developed in a paleovalley (Ciulli, 2005, Fig. 1).

The local substrate of the Buca dei Corvi section consists of Upper Jurassic serpentinite (Bartoletti et al., 1985). According to the revised stratigraphy proposed by Ciulli (2005) and shortly presented in this work, the Late Quaternary section can be divided into 11 different lithostratigraphic units (LU) (Fig. 2), which are, from the base to the top:

LU1 (10-11.80 m) – Deposit composed by layers of grey and light brown coarse-grained sand, and very coarse-grained sands with marine mollusc shells and well-rounded pebbles. In this unit, Blanc (1953) and more recently Nisi et al. (2003) found fossil remains of warm molluscan faunas. According to Hearty et al. (1986) LU1 belongs to aminozone E, correlated with MIS5e. Consistently, Mauz's (1999) OSL data yielded an age >108 ka.

LU2 (11.80-12.10 m) – It is composed by very red massive-silty sand, with the base containing strongly altered bioclasts and litharenite fragments from LU1. It can be interpreted as a well developed paleosol (Zembo et al., in progress).

LU3 (12.10-15.50 m) – Fine-yellow and light-brown cemented sand, with tangential cross stratification and convolute bedding and a pin-stripe lamination with foraminifer fragments (aeolian).

LU4 (15.50-20.60 m) – Cemented sands characterized by low-angle cross and concave stratifications, with rounded pebbles and marine mollusc fragments. At the top of this unit there are evident carbonate concretions indicating sub-aerial exposure. The LU4 and LU3 have been dated by Mauz (1999) at 94±34 ka, which still indicates the late MIS5.

LU5 (20.60-22.00 m) – Massive red silty sands with dispersed pebbles (palaeosol).

LU6 (22.00-22.50 m) – Cemented sand level with subvertical carbonate concretions (aeolian deposits?).

LU7 (22.50-25.00 m) – Clast-supported breccia with ophiolite clasts, faint stratification and fine-grained matrix.

LU8 (25.00-29.00 m) – A yellow-orange massive fine-silty to fine-sand deposit with small carbonate concretions and non-marine molluscs. The LU8 corresponds to the "loess" unit of Ottman's (1954) stratigraphy.

LU9 (29.00-29.50 m) – At the top of LU8 there is a darker brown massive silty-sand with non-marine molluscs and rare small rounded clasts.

LU10 (29.50-32.90 m) – Deposit with low-angle planar cross and concave stratification, formed by red silty-sand fining upward layers to very thick sandy layers, with oriented and concentrated pebbles at the base. The origin of this layer is not very clear. According to Ottman (1954) this represents reworking of loess. Mauz (1999) dated LU10 sediments with OSL at 9.7±2.4 ka and interpreted them as backshore deposits.

LU11 (32.90-33.70 m) – Present soil.

Overall, this stratigraphic reconstruction is generally consistent with that proposed by Ottman, (1954) and with the less detailed stratigraphy proposed by Mauz (1999). Fig. 2 shows the general stratigraphy with the OSL dates of Mauz (1999). The subjects of our discussion are LU9 and LU8.

3.Material and methods

Different levels were sampled over the LU8 and LU9 for lithological, geochemical, isotopic, paleontological and pedological investigations (Figs. 3, 4). Before sampling the surface was excavated for some tens of centimetres to reach the fresh deposit.

3.1 Sedimentological and geochemical analyses

Samples were collected discontinuously starting from ca. 25 m a.s.l., close to the base of the LU8, up to the very top of LU9 (Fig. 3). Subsamples of ca 0.5 kg were dried in an oven at 105 °C for 24 hours and then powdered. The powders were analysed using X-ray diffraction (XRD) for determining the main mineralogical phases, and with the XRF method for major oxide composition and trace element contents. The carbonate content of the samples was determined through gasometry (with calibration to pure calcite) as described by Leone et al. (1988). Replicate analyses show a mean reproducibility ca. ±5% (usually over a set of three replications). Part of the remaining

138 samples were sieved mechanically and fractions of >1 mm and >0.5 mm were inspected under a
139 binocular microscope. From these fractions carbonate concretions were selected. Carbonate
140 concretions were cleaned in an ultrasonic bath using deionized water, dried, powdered, checked for
141 mineralogical composition using XRD, and then analysed for oxygen and carbon stable isotopes.
142 The samples were analysed at SUERC (East Kilbride, Scotland) with an AP2003 mass spectrometer
143 equipped with a separate acid injector system, after reaction with 105% H_3PO_4 under He
144 atmosphere at 70 °C. The isotopic results are reported using the conventional δ‰-notation, relative
145 to V-PDB; $\delta^{18}O$ values of water are quoted relative to V-SMOW. Mean analytical reproducibility
146 (±1σ) was ±0.08‰ and ±0.10‰ for carbon and oxygen, respectively. During the period of analyses,
147 samples of internal laboratory standard (Carrara Marble) calibrated against NBS19 yielded a
148 reproducibility (±1σ) of ±0.07‰ and ±0.08‰ for carbon and oxygen respectively. For each level
149 three different concretions were analysed. Several modern pedogenic concretions were collected in
150 the area and analysed for comparison with old carbonate concretions isotopic data. They consist of
151 cylindrical carbonate concretion formed around roots (living and/or decaying, in the latter case roots
152 were still recognisable and related to present soil). According to Klappa (1980), they can be called
153 rhizoconcretions (Fig. 4B). Table 1 shows all the results for LU8-9, and Table 2 for the modern
154 pedogenic carbonates.
155 The entire succession is virtually devoid of significant organic matter remains and attempts for
156 dating were focused on carbonate concretions. Concretions from two different layers were analysed
157 by AMS ^{14}C dating technique at Beta Analytic (Florida USA, Table 3). Samples were previously
158 washed in a mixture of deionized water and H_2O_2 and then etched with diluted HCl for a few
159 seconds, to eliminate possible superficial carbonate contamination. Calibration was performed using
160 the INTCAL13 database (Reimer et al., 2013). Ages obtained on this kind of material may have
161 some limitation because of possible contamination by old carbonates (difficult to detect even after
162 careful selection), because of possible hard-water effects, and because of possible processes of
163 dissolution/re-precipitation of $CaCO_3$ (Budd et al., 2002). Moreover, carbonate concretions in loess
164 are not necessarily synchronous with loess deposition, then representing a minimum age of the
165 deposits (Gocke et al., 2011).
166
167 *3.2 Paleontological analyses*
168 Two samples of ca. 5 kg were selected for the fossil study in LU8 and LU9 respectively. They were
169 dried in an oven for 2 days at 40 ºC, then the sediment was disaggregated using a very dilute
170 solution of H_2O_2 and deionised water (ca. 5%). The material was then sieved using 2000, 1000, 500
171 and 250 µm mesh screens. All the identifiable shells and fragments were picked out under a

172 binocular microscope and counted using the convention of Sparks (1961) where every gastropod
173 apex is recorded to give a minimum number of individuals present. As adopted in the earliest
174 studies on the assemblages of terrestrial fossil mollusc of the Italian peninsula (e.g. Esu, 1981;
175 Crispino and Esu, 1995; Di Vito et al., 1998; Zanchetta et al., 2004, 2006; Esu and Gianolla 2009),
176 taxa were subdivided into ecological groups according to the scheme proposed by Ložek (1964;
177 1986; 1990; 2001).
178
179 *3.3 Paleopedological analyses*
180 The weathering profile was described in the field following Sanesi (1977) and sampled for bulk and
181 micromorphological analyses. The horizon nomenclature follows the terminology of the
182 internationally accepted guidelines proposed by FAO (2006). A Munsell Soil Color Chart was used
183 to determine soil colour on dry samples. For the micromorphological study, an undisturbed oriented
184 block was collected in the LU9 with Kubiëna box (Fig. 3). The thin section was prepared by the
185 *Laboratorio per la Geologia*–Piombino (Livorno, Italy) following the procedure of Murphy (1986).
186 The thin section, 120x90 mm, was observed with a polarizing transmitted light microscope under
187 plane (PPL) and cross polarized light (XPL) and described according Bullock et al. (1985) and
188 Stoops (2003, 2007); moreover, some concepts of Brewer (1964) were also taken into account and
189 the interpretation of micromorphological features was carried out following Stoops et al. (2010).
190 The origin and palaeoenvironmental significance of the weathering profile is mainly based on
191 micromorphological observations.
192
193 **4.Results**
194
195 *4.1 Field and pedological observations*
196 The outcrop section here described, about 9 m thick, is representative of the topmost units (from
197 LU8 to LU11, the present soil) of the Buca dei Corvi cliff–section, and was described along the
198 S.S.1-Aurelia starting from at an elevation of about 25 m a.s.l. (Fig. 2,3). LU10 is ca. 250 cm of
199 coastal eolianite to colluvial deposits on top weathered by a recent soil cover (LU11; Fig. 3 A,B).
200 The LU10 deposits are constituted by planar and trough cross–laminated sands, with alternating fine
201 and coarse laminae; subangular fine pebbles are locally concentrated at the base of the laminae,
202 often showing an erosive basal surface. LU10 is separated from LU9 by a clear erosional surface.
203 The LU9 is essentially sandy loam in texture, and consists of a massive and bioturbated calcic
204 horizon Bk, about 60 cm thick, marked by dull yellowish brown to yellow orange matrix colours
205 (Munsell color: 10YR 5/4–6/4; Fig. 3a), and a high frequency of coarsely-cemented pedogenic

concretions (Munsell color: 2.5Y 7/4). Carbonate concentrations (millimetres in size) are dispersed throughout the matrix. This horizon is characterised by moderately developed prismatic to sub–angular blocky structure with hard rupture resistance. The coarse (ϕ_{max}= 5 mm) and angular rock fragments that do occur in this horizon are serpentinite clasts. Rare non–marine molluscs are also preserved. As reported above, the upper limit of the Bk horizon is abrupt and indicates an erosional surface truncating the topsoil horizons. The transition between the Bk horizon and the lower and thicker (350 cm) LU8 is clear. The features of LU8 are broadly similar to those of LU9 except for the pale-yellow matrix colour (Munsell color: 2.5Y 7/4–6/4) and for the scarcer presence of scattered clasts. This unit is characterised by a 2BCk horizon with well-developed angular and sub–angular blocky structure passing downward into 2Ck horizon. Rhizoconcretions are present only in the 2BCk horizon. In comparison to the overlying Bk horizon (LU9), it has perceptible silt content, and is particularly indurated (transition to petrocalcic horizon). The deepest part of the LU8 can be considered as a transition to saprolite. The lower boundary of LU8 is not exposed at the base of the studied outcrop section.

4.2 Micropedology

In thin section, the Bk horizon (LU9) is apedal with close to single spaced porphyric patterns, locally chito-gefuric (Fig. 5A–H). The microstructure is controlled by voids (Fig. 4A). The porosity pattern is dominated by channels (root and faunal), and subordinately by chambers and simple packing voids; estimated total void space is 25-30%. The silty clay micromass has a dull yellowish brown colour (PPL) with some local yellowish and dark mottles (Fig. 5B), and cloudy to opaque appearance. The crystallitic b–fabric is combined with an undifferentiated b–fabric (Fig. 5E–H); locally mono– and granostriated b–fabrics occur. Well-sorted and dominantly subangular quartz grains dominate the coarse fraction (>10 μm); they are accompanied by feldspar (plagioclase), muscovite and rare biotite minerals, generally weakly weathered. Heavy minerals are rare. Compound mineral grains and rock fragments are frequent; they include medium– and coarse–sand sized polycrystalline quartz (Fig. 5E) and metamorphic rock fragments (serpentinite). A few mollusc fragments, partially weathered, were observed (Fig. 5A and C). Iron and iron–manganese oxides occur as impregnative features (segregation into the soil matrix, nodules, hypo- and quasicoatings). Typic and rare geodic nodules of different size (20 μm–1 mm in diameter; Fig. 5A, B) are orthic, dark brown, moderately to strongly impregnated, and generally irregular. Rare anorthic nodules have a sharp boundary with the soil matrix and dark brown colours (Fig. 5F); they are probably inherited by the erosion of a former weathered horizon or paleosol (Brewer, 1976). Calcite crystalline pedofeatures are segregated into frequent and large (160 μm to millimetre diameter) intrusive infillings (dense incomplete and loose discontinuous), distributed throughout the

Bk horizon, and are juxtaposed with brownish redoximorphic features. They are composed by equigranular anhedral micritic crystals and are located mainly in channels and large voids. Crystalline micritic impregnative hypocoatings occur on voids (mainly on root channels, see examples in Durand et al. 2010) together with coatings of mineral grains, rock and mollusc fragments. Textural pedofeatures are rare (≤ 2%) and show various indications of degeneration (fragmentation, assimilation into the soil matrix). Three types of fragmented clay coatings (i.e. papules, according Brewer, 1976) were observed: the first two are dusty, non-laminated, red and orange yellowish in colour respectively (Fig. 5C, D, E and H). Their extinction patterns are virtually absent. The third pure clay coatings are yellow and show sharp extinction bands between crossed polarizers (XPL).

4.3 Chemistry and mineralogy

XRD and binocular microscope observations on different fractions, in agreement with micropedology and pedological observations, show that the samples collected from LU8 and LU9, are mainly composed by quartz, calcite and a minor amount of plagioclase, feldspar and micas. The calcite is mostly due to the presence of pedogenic carbonates. According to Retallack (1990) these carbonates can generally be called calcareous rhizoconcretions and calcareous glaebules (Brewer, 1964) or nodules (Bullock et al., 1985). More specific, sometime confusing, literature exists on the description and genetic origin of pedogenetic carbonate in soil/loess profiles (e.g. Klappa, 1980; Barta, 2011 and reference therein). The most abundant pedogenic carbonate identified in LU8 and LU9 resembles "hypocoatings" (Fig. 4C, Barta, 2011). Hypocoatings indicate dry formation environments and have probably the same age as the dust accumulation (Barta, 2011) and their presence may refer to former patchy vegetation. The higher carbonate concentration could cement hypocoatings together, which will act like a nucleus for later precipitation producing larger concretions (i.e. nodules).

Qualitatively, the observations under binocular microscope showed that the basal samples are coarser and contain arenitic clasts, rare eroded and partially altered small bioclast fragments of marine molluscs and forams, and a minor amount of ophiolite clasts derived by the dismantling of the substrate. These virtually disappear progressively upward and are completely substituted by a fine-grained matrix dominated by angular to poorly rounded quartz grains, with rare land snail shells, and with the carbonate fraction ranging from ca. 5 to 40 % (Fig. 6), with the lower values found in the LU9.

The CaO and $CaCO_3$ contents (Fig. 6) show a high degree of correlation (R^2=0.99), which implies CaO is mainly related to calcite precipitation and not from the bedrock (e.g. anorthitic plagioclase

and Ca-pyroxene). TiO_2-MnO-Fe_2O_3 are highly correlated, as are Fe_2O_3 and transition metals (V, Cr, Co) (Fig. 6); because transition metals can be hosted in Fe-Mn-oxides, the transition metal concentration can indicate the relative abundance Fe-Mn-oxides. However, the positive correlation between Fe_2O_3 and MgO (R^2= 0.92) can also indicate that these phases are probably related to the variation of the content in the substrate rocks.

$CaCO_3$-Sr are positively correlated (R^2=0.91) indicating that Sr is principally hosted in the $CaCO_3$ concretions. Ba and Sr are instead negatively correlated (R^2=0.86). This may be due to the different partition coefficients of these trace element related to $CaCO_3$ for the progressive evolution of the solution into the soil, dissolving and precipitating carbonate (Morse and Bender 1990), but it can also be due to the fact that Ba could be mostly related to the mafic substrate. All these data indicate the presence of a local clastic source, and an "exotic" one related, for instance, to abundant quartz, and a secondary chemical deposition (pedogenic) related to $CaCO_3$ precipitation. The carbonate can be directly precipitated by chemical weathering of Ca-rich minerals (e.g. White et al., 1999; Knauth et al., 2003) but in the absence of carbonate rocks it can be related to the arrival of externally-sourced carbonate, transported by winds (the so-called primary carbonate of loess deposits, Pécsi, 1990), which is then progressively dissolved/re-precipitated during pedogenetic processes.

4.4 Stable isotopes

Modern pedogenetic carbonates sampled in two localities along the Tuscan coast show a relatively narrow isotopic variability (Figs. 1, 4A, 6; Table 2). The $\delta^{13}C$ ranges from -9.5 to -10.6 ‰ (mean -10.2±0.3 ‰), whereas $\delta^{18}O$ ranges from -3.7 to -4.9 ‰ (mean -4.4±0.4 ‰). However, the two sites show a small difference in their oxygen isotope values (ca. 0.7 ‰) possibly indicating small differences in soil water evaporation with an ^{18}O-enrichment in the soil solution at Castiglioncello (e.g. Cerling and Quade, 1993; Zanchetta et al., 2000). Significant differences in the mean temperatures can be ruled out, as well as local differences of the isotopic composition of meteoric precipitation (Longinelli and Selmo, 2003), which is quite constant along the Tyrrhenian coast and around -5 ‰. The carbon stable isotope composition is in the range expected for soil supporting a C_3 plant community (Cerling and Quade, 1993). Pedogenic carbonates in LU8 show a $\delta^{13}C$-$\delta^{18}O$ positive correlation (R^2=0.76), with $\delta^{13}C$ ranging from -5.8 to -8.9 ‰ (mean -7.6 ±1.0 ‰) and $\delta^{18}O$ ranging from -4.4 to -2.5‰ (mean -3.5±0.6 ‰). These figures indicate that important differences exist between modern pedogenic carbonates and those within LU 8 (Figs. 4A, 6). Moreover, along the section there is a clear and consistent variation, with higher $\delta^{13}C$ and $\delta^{18}O$ values between 28,8 and 20 m a.s.l.

4.5 The non-marine mollusc assemblage

The non-marine mollusc assemblage is strongly oligotypical (e.g. Esu et al., 1989) and comprises only four species of Gastropod pulmonata: *Pupilla muscorum* (LINNEUS 1758), *Vallonia pulchella* (MÜLLER 1774), *Candidula unifasciata* (POIRET 1801) and *Jamina quadridens* (MÜLLER 1774). Because no significant changes occurred between different samples, we consider the total of all samples. Number of specimens and percentages are reported in Table 4.

ECOLOGICAL GROUP 4 – STEPPE

This group includes the species which inhabit dry and sunny places like *Candidula unifasciata* and *Jamina quadridens*. According to Adam (1960), Magnin (1993), and Kerney and Cameron (1999) *C. unifasciata* is characteristic of dry, open rocky areas including dunes. It reaches 2000 m of altitude in the Alps (Kerney and Cameron, 1999). Studies on French populations report *C. unifasciata* as a "continental" species, avoiding typical Mediterranean climate (Pfenninger and Magnin, 2001; Pfenninger et al., 2003).

Jaminia quadridens is a xerophilous species which lives in sunny and open lands, upon herbaceous and shrubby vegetation, especially on calcareous rocks. It is not very common in grassland with a principal distribution over the Mediterranean (Kerney and Cameron, 1999).

This group is the most dominant, accounting for 80% of the assemblage, with *C. unifasciata* alone accounting for 79% of the specimens.

ECOLOGICAL GROUP 5 – OPEN LANDS

This group includes the species living in open lands but with different requirements in terms of humidity (Ložek, 1964, 1990). *Vallonia pulchella* is typical of open calcareous habitats, moist meadows, marshes sand dunes and occasionally dry grasslands and screes (Kerney and Cameron, 1999). *Pupilla muscorum* is common in open spaces such as dry exposed calcareous places: screes, stones walls, grassland, dunes (Adam 1960; Kerney and Cameron, 1999). It is commonly believed to be resistant to low temperature and is frequently found in Pleistocene loess deposits of Central Europe (Ložek, 1964, 1990; Puisségur 1976; Esu et al. 1989).

4.6 Chronology

OSL ages from Mauz (1999) and our ^{14}C dating are in agreement and indicate that this succession is probably of Late Glacial age, being constrained by the basal coastal marine layers grossly corresponding to late MIS5, and the age of the LU10 dated at 9.7±2.4 ka by luminescence methods. The two radiocarbon dates were obtained on carbonate concretions, appear in stratigraphic order and suggest an age which may overlap with Late Allerød and Younger Dryas (YD) (Table 3), or better with the GS -1 and GI-1 (Björck et al., 1998; Blockley et al., 2014). It is often assumed that pedogenic carbonates in loess successions are formed synchronously with loess deposition but radiocarbon dating of loess-paleosoil sequences have shown that this is not necessarily the case (Gocke et al., 2011). Therefore, in the later discussion is implicitly assumed that these radiocarbon dating represent a minimum age for the deposits. Then, stable isotope composition of pedogenic carbonates can give information at the time constrained by radiocarbon dating, but not necessarily coincident with the time of loess deposition.

5.Discussion

The succession has a substrate formed by ophiolitic rocks, and the presence of abundant quartz and white and black micas clearly indicates an external source of clastic material. One possible source for these minerals would be the arenitic Macigno Formation extensively outcropping along this sector of the coast (Lazzarotto et al., 1990). Given the local geomorphological conditions they can, however, only be supplied by wind transport. Figure 7 shows the comparison between composition of the Macigno Formation and LU9 and LU8 units for SiO_2-Al_2O_3-CaO and Fe_2O_3-MnO-TiO_2 diagrams. It is evident they show significantly different compositions, representing the mixing of different sources, even although the Macigno Formation probably represents one of the sources forming the LU9 and LU8 units (e.g. Fig 7, SiO_2-Al_2O_3-CaO diagram). A second source could have originated by the local dismantling of the littoral arenites from the lower unit part of Buca dei Corvi sections. LU4 is basically aeolian and the deposits of this unit could have outcropped well above the present sea level. Indeed in the lower part of the analysed section, fragments of this unit are present. However, tiny fragments of marine shells and clasts of the lower arenitic units are restricted only to the two lower samples and disappear upwards. Therefore, dust transportation by wind is a reasonable origin, even if the coarser fraction would have been supplied by local colluvium along the slope from the local mafic bedrock.

In light of previous discussion, LU9-LU8 buried horizons reflect the land surface aggradation, which occurred in a Mediterranean coastal area through both eolian and colluvial deposition,

progressively affected by pedogenic processes. The truncated upper limit indicates that soil-forming processes were followed by an erosional phase, in agreement with the nature of the upper LU10.

The macromorphological and micromorphological analyses reveal that the main soil-forming processes were characterized by calcite migration, re-precipitation and accumulation, so that the LU9 horizon can be generically regarded as "Calcisol" (IUSS Working Group WRB, 2006). Calcium carbonate-rich horizons are common in highly calcareous parent materials and widespread in arid and semi-arid environments (IUSS Working Group WRB, 2006), indicating higher annual evaporation and low annual precipitation. On the Earth surface today calcic soils develop in areas receiving less than 1000 mm yr^{-1} precipitation, with the great majority in areas of less than 800 mm yr^{-1} precipitation (Buck and Mack, 1995, Retallack, 2005). In addition, the presence of redoximorphic features in the LU9 horizon points to a "short" period of water saturation (Lindbo et al., 2010) and suggests that precipitation may have been seasonal (Buck and Mack, 1995). Fragments of illuvial coatings occur in transported material or in soils with strong bioturbation (Kühn et al., 2010): in this light it is possible to state that clay illuviation can be regarded as an indicator of a former pedogenic phase taking place in a past environmental context, prior both to pedoturbation (responsible for fragmentation of clay coatings) and to development of calcic features (which are not compatible with clay dispersion required for clay illuviation, Kühn et al., 2010 - see also Zerboni et al., 2011 for a similar sequence of processes).

The studied weathering horizon LU9 exhibits distinct evidence of relict soil processes that can be referred to climatic conditions very different from the present; hence it can be considered as a buried paleosol according to the Paleopedology Glossary by the INQUA Working Group on "Definitions used in Paleopedology" (1995). The fact that the substrate is not carbonate is a further argument for eolian deposition of carbonate, which is subsequently re-deposited along the soil profile.

Non-marine faunal assemblage analysis complements the pedological observations. Overall, the association indicates the presence of an open and dry area, probably with climate conditions colder than the present day. This kind of association characterizes the cold and arid phases of the Middle to Late Pleistocene in Central and Southern Italy (Esu, 1981; Esu et al., 1989; Esu and Girotti, 1991; Di Vito et al., 1998; Marcolini et al., 2003; Sarti et al., 2005) and shares some common characteristics with cold and arid phases of loess deposition of Europe (e.g. Ložek, 1964, 1990, 2001; Puisségur, 1976; Limondin-Lozouet and Antoine, 2001). However, the climatic indication is not as extreme as in Central Europe given the presence of more thermophilous Mediterranean elements like *J. quadridens.*

411 Although we have to take into account that radiocarbon ages of pedogenic carbonates can be
412 susceptible to several concerns such as incorporation of old carbonate and/or dissolution and
413 carbonate redeposition, and the possible absence of contemporaneity of pedogenic carbonate with
414 the deposit, the dates reported here are generally consistent with the hypothesis that most of LU9-8
415 would have developed during the Late Glacial (Table 3). This is further constrained by the OSL
416 date of 9.7±2.4 (Maunz, 1999) from LU10.
417 Regional arboreal pollen reconstructions indicate during the Late Glacial a larger presence of
418 vegetation typical of open spaces compared to the Holocene (Fig. 8, e.g. Ramrath et al., 2000;
419 Brauer et al., 2007; Allen and Huntley, 2009).
420 Qualitatively, the oxygen isotopic composition of pedogenic carbonate from LU8 and LU9 is
421 generally ^{18}O-enriched compared to present day-forming pedogenic carbonate in coastal Tuscany.
422 As reported for other continental carbonates forming in different Mediterranean regions (e.g.
423 Zanchetta et al., 2000, 2005; 2006, 2007a,b, 2015; Roberts et al., 2008; Regattieri et al., 2014, 2015,
424 2016), high $\delta^{18}O$ values can be associated to dry conditions. This can be related to several factors in
425 combination, including increasing evaporation (e.g. Zanchetta et al., 1999; 2000, 2007a; Roberts et
426 al., 2008), decrease in the amount of precipitation (Bard et al., 2002; Zanchetta et al., 2007a,b,
427 2014; Regattieri et al., 2015, 2016) and/or changes in the provenance of the precipitation (Zanchetta
428 et al., 2007a,b).
429 Using Cerling's (1984) data on modern soils, Jiamao et al. (1997) proposed the following
430 relationship between $\delta^{18}O$ values in water and soil carbonate, which incorporates the evaporative
431 effect in soils (Zanchetta et al., 2000):
432
433 $\delta^{18}O_{H2O} = -1.361 + 0.955\ \delta^{18}O_{CaCO3}$ ($R^2 = 0.98$)
434
435 Overall, modern soil carbonates of this study (data in Table 2) yield $\delta^{18}O_{H2O}$ of -5.6± 0.4 ‰, which
436 is in very good agreement with modern rainfall $\delta^{18}O_{H2O}$ values observed along the Tyrrhenian coast
437 of Italy (ca. -5.5 ‰; Longienelli and Selmo, 2003). Our results indicate that Jiamao's equation is a
438 robust predictor of $\delta^{18}O_{H2O}$ values also for the studied area. The $\delta^{18}O_{H2O}$ values for LU8 and LU9
439 carbonates range from -3.9 ‰ to -5.5 ‰, with an average value of -4.7±0.6 ‰. On average, this
440 implies meteoric waters enriched by ca. 1 ‰ compared to present day. Bard et al. (2002) reported
441 for the area an amount effect in precipitation of ca. -2 ‰/100 mm/month for the oxygen isotopic
442 composition, which in our case could indicate a decrease in precipitation of ca. 50 mm/month for
443 the period. However, this estimate does not incorporate changes in the average $\delta^{18}O$ values of the
444 oceans due to variations in the ice volume during deglaciation (the so-called source effect). For

example, according to Lambeck et al. (2014) the eustatic sea level for the considered time interval would have ranged from ca. -40 to ca. -80 m below present day sea level (Fig. 8, Lambeck et al., 2014). Using a coefficient of 0.009 ‰/m^{-1} for the effect of eustatic sea level on the average $\delta^{18}O$ value of oceans (Lambeck et al., 2014; Rohling et al., 2014; Shakun et al., 2015), a sea level stand between ca. -40 to -80 m would have promoted a change in the average $\delta^{18}O$ value of the oceans of from +0.36 ‰ to +0.72 ‰. This may suggest that part of the isotopic enrichment could be due to changes in the isotopic composition of the oceans. We have also to consider that the Mediterranean is a "concentration" basin in which the isotopic composition of sea water is higher than the ocean average (Pierre, 1999; Emeis et al., 2000). However, isotopic data (Figs. 6,8), are not consistent with a significant source effect. This would be expected to be more pronounced for the lower (and so older) samples, which is not the case. Therefore, $\delta^{18}O$ values are most likely indicative of drier conditions, characterised by higher $\delta^{18}O$ in meteoric precipitation probably related to decrease in the amount of precipitation.

The average value of the $\delta^{13}C$ of modern pedogenic carbonate is -10.2±0.3 ‰, significantly lower than Late Glacial pedogenic carbonate (-7.6±1.0 ‰). This difference can be due to different factors. Indeed, the carbon isotope composition of pedogenic carbonates ultimately derives from the isotopic composition of soil CO_2, which depends on soil respiration rate and the amount and typology of vegetation (Cerling and Quade, 1993). Therefore, higher values are consistent with lower respiration rate and/or changes in the proportion of C_3/C_4 and/or simple changes in ratio between shrubs/herbs/trees, with trees having usually the lower isotopic composition (e.g. Masi et al., 2013a,b). Lower respiration rate and increase in C_4 are both indicators of drier conditions (Raich et al. 1992), even though C_4 are also adapted to higher temperature (Deines, 1980).

According to Wang and Zheng (1989) the proportion of C_4 plants (x) can be calculated using the equation:

$$x = (11.9 + \delta^{13}C_{CaCO3})/14$$

According to this calculation, the Late Glacial would be characterized by larger proportion of C_4 vegetation (ca. 30%) compared to present day (ca. 11%). For instance, this could be due to the increase of grass and sedge, which include species having C_4 photosynthesis in particular in Amaranthaceae and Chenopodiaceae (e.g. Ehleringer et al., 1997).

However, these estimations are based on the assumption that C_3 plants have a mean carbon isotopic value of ca. -27 ‰, whereas in the Mediterranean C_4 vegetation is rare and restricted to some specific environments (Colonese et al., 2014), and carbon isotopic composition of C_3 vegetation in

drier environments can be significantly higher than the average (e.g. Kohn , 2010; Diefendorf et al., 2010; Masi et al., 2013a,b). In the Mediterranean, significant differences are observed in water-use efficiency which varies largely between evergreen and deciduous species (e.g. Valentini et al., 1992) and also seasonally (Filella and Peñuelas, 2003). So the estimation of the amount of C_4 is probably too high. Breecker et al. (2009) observed that pedogenic carbonates in dry environments form during warm, dry periods and do not record mean growing season conditions as typically assumed. Therefore, pedogenic carbonate provides a C_4-biased record of paleovegetation, especially in dry soils. Accordingly, higher values recorded in the LU8 and LU9 units compared to present pedogenic carbonates reasonably indicate soil conditions characterized by lower respiration rate in a drier climate (e.g. Raich et al. 1992), with vegetation composition different from present conditions. However, a comment is necessary for the high linear correlation observed between $\delta^{13}C$-$\delta^{18}O$ in Late Pleistocene carbonates (Fig. 4, R^2=0.76). If also modern data are included the correlation still appears high (R^2=0.71). This high correlation can be explained in different ways. Considering that the regression line has equation for LU8 and LU9:

$$\delta^{13}C=0.506\ \delta^{18}O + 0.323$$

this means that the regression line passes close to the origin of the axes with an isotopic composition resembling that of marine carbonate (e.g. Land, 1989). Therefore, a mixing with a clastic marine component could be possible. Assuming a simple mixing model with two end members: the isotopic composition of marine carbonate (close to 0‰) and the modern "pure" pedogenic carbonate composition, the highest values of late Pleistocene pedogenic carbonate would be produced by a mixing ratio of ca. 50% with marine carbonate. Different values would be obtained using a higher isotopic composition of the clastic marine component (Land, 1989). In any case, if the clastic contamination were so high, any calculation of past vegetation and/or isotopic composition of meteoric water would be unreliable. However, this scenario is unlikely. Indeed, there is no evidence of so large a clastic carbonate amount in the sediment: very rare marine fragments in the >1 mm fraction are observed only at the base of the outcrop. No other clastic carbonate was detected. Moreover, if fragments of marine shells were the source of contamination, this would be detected by the presence of traces of aragonite in the XRD, which is not the case; and finally, petrographic observation did not support large amounts of clastic carbonate.

A more likely explanation for the isotopic covariation is related to the climatic effect. For instance it has been observed in speleothems of central Italy that $\delta^{13}C$-$\delta^{18}O$ positive correlation can be driven by climatic effects (e.g. Drysdale et al., 2004; Zanchetta et al., 2007a,b, 2015; Regattieri et al.,

2014a,b). Increasing carbonate $\delta^{13}C$ and $\delta^{18}O$ values are related to decrease in precipitation and decrease of CO_2 production in soils for the drier conditions. Moreover, low respiration rate in drier environments can favor a deeper penetration of atmospheric CO_2 within the top soil (Cerling and Quade, 1993). Low precipitation, as discussed earlier, can produce organic matter with higher $\delta^{13}C$ values, as well as higher $\delta^{13}C$ values of respired CO_2. A positive correlation, even if mediated by other factors, has also been observed in lacustrine carbonate of the same region and interpreted as changes in soil productivity during drier and colder intervals accompanied by higher $\delta^{18}O$ values of water for changing composition of meteoric precipitation and increasing evaporation (Regattieri et al., 2015, 2016; Giaccio et al., 2015).

Despite potential limitation of accuracy and precision related to the material dated, the available chronology consistently indicates that LU8 and LU9 may have formed during the Late Glacial, in drier conditions compared to present day. For this period pollen data from Monticchio (Brauer et al., 2007), oxygen isotope composition from Corchia cave (Zanchetta et al., 2007b; Regattieri et al., 2014) and sea surface temperature from ODP976 (Martrat et al., 2014), suggest more drier and colder condition than in the Holocene (Fig. 7). These data are compared to the NGRIP record as extra-regional reference data. Over the central Apennine area loess deposition is interrupted with the onset of the Bølling-Allerød time interval, as constrained by tephra layers (Giraudi et al., 2013, Fig. 8). We can speculate that the possibility of dust accumulation on the coastal area for a longer period compared to the Apennine is probably related to the fact that the continental platform was still exposed by the low sea level stand (Fig. 8), representing the deflation area for the sediment, in a context where vegetation and soil had not completely recovered.

6.Summary and Conclusions

Lithological, pedological and geochemical data support the presence of pedogenically altered loess deposits at the top part of the Buca dei Corvi succession as reported by Ottman (1953). These deposits were partially colluviated and mixed with fragments originating from the local substratum. Chronologically (at least for the exposed part) they likely have accumulated during the Late Glacial and/or experienced pedogenic alteration during this period. Non-marine mollusc assemblage, pedogenic features and stable isotopes of pedogenic carbonates indicate environmental conditions drier than the present day and characterized by sparse vegetation. Using the $\delta^{18}O$ values of modern pedogenic carbonates for calculating present day $\delta^{18}O$ values of meteoric precipitation with the Jiamao et al. (1991) equation, yielded values consistent with measured local meteoric precipitation, indicating that this equation is robust also for the area and useful for reconstructing quantitatively

546 past isotopic composition of rainfall. Carbon isotopic composition indicates a higher proportion of
547 C_4 plants (possibly related to an increase of herbs in vegetation) and/or decrease in soil respiration
548 rate. An increase in the isotopic composition of C_3 vegetation component due to more hydrological
549 stress could also have produced ^{13}C-enriched soil organic matter and then a more ^{13}C-enriched soil
550 CO_2 (Deines, 1980).
551 Most of the raised-marine terraces over the Tyrrhenian coast have been simply utilized for
552 reconstruction of relative high stand paleosealevel and/or tectonic movement with respect to a
553 certain expected eustatic sea level (e.g. Mauz, 1999; Nisi et al., 2003). This work has demonstrated
554 that more information can be obtained for characterizing low stand conditions and climate
555 deterioration, and the terraces can be useful archives for reconstruction of coastal evolution.
556 Moreover, this work suggests that distribution of loess deposits can be extended in the future to the
557 Tyrrhenian coast, in a more southerly position than previously documented.
558
559 **Acknowledgments**
560 This research has been funded by University of Pisa (Fondi di Ateneo, Leader G. Zanchetta). GB
561 thanks the *Ministero degli Affari Esteri* of Italy for supporting her research with a six-months grant.
562 SUERC is funded by a Consortium of Scottish Universities and NERC. This publication was also
563 developed within the frame of University of Pisa PRA 2015 project (Leader G. Zanchetta) and
564 CICTERRA-CONICET (Argentina) for studying the coastal area evolution of Patagonia and Italy.
565 We thank and anonymous review and F. Scarciglia for the comments, which greatly improved the
566 quality of the final manuscript.
567
568 **References**
569
570 Adam, W., 1960. Mollusques terrestres et dulcicoles. Faune de Belgique. Institut royale des
571 Sciences naturelles de Belgique. Bruxelles, 402 pp.
572
573 Allen, J.R.M., Huntley, B. 2009. Last Interglacial palaeovegetation, palaeoenvironments and
574 chronology: a new record from Lago Grande di Monticchio, southern Italy. Quat. Sc. Rev., 28,
575 1521-1538.
576
577 Bard, E., Delaygue, G., Rostek, F., Antonioli, F., Silenzi, S., Schrag, D.P. 2002. Hydrological
578 conditions over the western Mediterranean basin during the deposition of the cold Sapropel 6 (ca.
579 175 kyr BP). Earth Planet. Sc. Lett. 202, 481-494.

Barta, G. 2011. Secondary carbonates in loess-paleosoil sequences: a general review. Centr. Europ. J. Geoscienc. 3/2, 129-146.

Bartoletti, E., Bossio, A., Esteban, M., Mazzanti, R., Mazzei, R., Salvatorini, G., Sanesi, G., Squarci, P. 1985. Studio geologico del territorio comunale di Rosignano Marittimo in relazione alla carta geologica 1:25.000. Quad. Mus. St. Nat. di Livorno 6, suppl. 1, 33-127.

Björck, S., Walker, M.J.C., Cwynar, L., Johnsen, S.J., Knudsen, K.L., Lowe, J.J., Wohlfarth, B., INTIMATE Members 1998. An event stratigraphy for the Last Termination in the North Atlantic region based on the Greenland Ice Core record: a proposal by the INTIMATE group. J. Quat. Sci. 13, 283-292.

Blanc, A.C., 1953. Plage tyrrhenièNne et dunes fossils de la Buca dei Corvi, Castiglioncello. Livret-Guide, IV Congr. Int. INQUA, 1953. Pisa.

Blockley, S., Rasmussen, S.O., Harding, P., Brauer, A., Davies, S., Hardiman, M., Lane, C., Macleod, A., Matthews, I., Wulf, S., Zanchetta, G. 2014. Tephrochronology and the extended INTIMATE (Integration of ice-core, marine and terrestrial records) event stratigraphy 8-110 ka B2K. Quat. Sci. Rev., 106, 88-100.

Breecker, D.O., Sharp, Z.D., McFadden, L.D. 2009. Seasonal bias in the formation and stable isotopic composition of pedogenic carbonate in modern soils from central New Mexico, USA. GSA Bulletin, 121, 630–640.

Brewer, R. 1964. Fabric and Mineral Analysis of Soils. Wiley, New York, 472.

Brewer, R., 1976. Fabric and Mineral Analysis of Soils. Robert E. Krieger Publishing Company, Huntington, New York, p. 482.

Buck, B. J. and Mack, G. H. 1995. Latest Cretaceous (Maastrichtian) aridity indicated by paleosols in the McRae Formation, south-central New Mexico. Cretaceous Research, 16, 559–572.

613 Budd, D.A., Pack, S.M., Fogel, M.L. 2002. The destruction of paleoclimatic isotopic signal in
614 Pleistocene carbonate soil nodules of Western Austalia. Palaeogeogr., Palaeoclimatol., Palaeoecol.,
615 188, 249-273.
616
617 Bullock, P., Fedoroff, N., Jongerius, A., Stoops, G., Tursina, T., Babel, U. 1985. Handbook for Soil
618 Thin section Description. Waine Research Publications, Wolverhampton, p. 152.
619
620 Cerling, T.E. 1984. The stable isotopic composition of modern soil carbonate and its relationship to
621 climate. Earth Planet. Sc. Lett. 71, 229–240.
622
623 Cerling, T.E., Quade, J. 1993. Stable carbon and oxygen isotopes in soil carbonates. In Climate
624 Change in Continental Isotopic Records, Swart PK, Lohmann KC, McKenzie JA, Savin S. (eds).
625 American Geophysical Union, Geophysical Monograph 78**,** 217–231.
626
627 Ciulli, L., 2005. Analisi di facies dei depositi tardo quaternari nel tratto costiero tra Livorno e
628 Piombino: implicazioni paleoambientali e neotettoniche. Tesi inedita, Facoltà SMNF, Università di
629 Pisa, 237 pp. (unpublished Masters thesis).
630
631 Colonese, A.C., Zanchetta, G., Fallick, A.E., Manganelli, G., Lo Cascio, P., Hausmann, N.,
632 Baneschi, I., Regattieri, E. 2014. Oxygen and carbon isotopic composition of modern terrestrial
633 gastropod shells from Lipari Island, Aeolian Archipelago (Sicily). Palaeogeogr., Palaeoclimatol.,
634 Palaeoecol., 394, 119–127.
635
636 Cremaschi, M. (ed) 1990. The loess in Northern and Central Italy: a loess basin between the Alps
637 and the Mediterranean region. Quad. Geod. Alpin. Quat., 1, 1-187, Verona.
638
639 Crispino, P., Esu, D. 1995. Non-marine Late Villafranchian molluscs of the Crostolo river (Emilia,
640 Northern Italy): systematics and paleoecology. Boll.Soc. Geol. It., 34, 283-300.
641
642 Deines, P. 1980. The isotopic composition of reduced organic carbon. In P. Fritz and J.Ch. Fontes:
643 Handbook of Environmental Isotope Geochemistry. 1, 329-406. Elsevier.
644

645 Diefendorf, A.F., Mueller, K. E., Wing, S.L., Koch, P.L., Freeman, K.H. 2010. Global patterns in
646 leaf ^{13}C discrimination and implications for studies of past and future climate. PNAS, 107, 5738–
647 5743.
648
649 Di Vito, M., Sulpizio, R., Zanchetta, G. 1998. I depositi ghiaiosi della Valle dei torrenti Clanio e
650 Acqualonga (Campania centro-orientale): significato stratigrafico e ricostruzione paleoambientale.
651 Il Quaternario, 11, 273-286.
652
653 Drysdale, R., Zanchetta, G., Hellstrom, J., Fallick, A.E., Zhao, J., Isola, I., Bruschi, G. 2004. The
654 palaeoclimatic significance of a Middle to late Pleistocene stalagmite from the Alpi Apuane karst,
655 central-western Italy. Earth Planet. Sc. Lett., 227, 215-229.
656
657 Durand, N., Curtis Monger, H., Canti, M.G. 2010. Calcium Carbonate Features. In: In: Stoops, G.,
658 Marcelino, V., Mees, F., (eds). Interpretation of Micromorphological Features of Soils and
659 Regoliths, Elsevier, pp 149-194.
660
661 Ehleringer, J.R., Cerling, T.E., Helliker, B.R. 1997. C_4 photosynthesis, atmospheric CO_2, and
662 climate. Oecologia, 112, 285-299.
663
664 Emeis, K.-C., Struck, U., Schulz, H.-M., Rosenberg, R., Bernasconi, S., Erlekeuser, H., Sakamoto,
665 T., Martinez-Ruiz, F. 2000. Temperature and salinity variations of Mediterranean Sea surface
666 waters over the last 16,000 years from records of planktonic stable oxygen isotopes and alkenone
667 unsaturation ratios. Palaeogeogr., Palaeoclimatol., Palaeoecol., 158, 259–280.
668
669 Esu, D., Girotti, O. 1991. Late Pliocene and Pleistocene assemblages of continental molluscs in
670 Italy. A survey. Il Quaternario, 4, 137-150.
671
672 Esu, D., Girotti, O., Kotsakis, T. 1989. Oligotopia nei vertebrati e nei molluschi continentali fossili.
673 Atti 3º Simposio di Ecologia e Paleoecologia delle Comunità Bentonitche, Catania-Taormina, 285-
674 298.
675
676 Esu, D. 1981. Significato paleoecologico e paleoclimatico di una malacofauna continentale
677 pleistocenica dell'Italia centro-meridionale (Iberni, Molise). Boll. Soc. Geol. It., 100, 93-98.
678

679 Esu, D., Gianolla, D. 2009. The malacological record from the Plio-Pleistocene Leffe Basin
680 (Bergamo, Northern Italy). Quat. Inter., 204, 11-19.
681
682 FAO 2006. Guidelines for Soil Description, Fourth edition. Food and Agriculture Organization of
683 the United Nations, Rome, Italy.
684
685 Federici, P.R., Mazzanti, R. 1995. Note sulle pianure costiere della Toscana. Mem. Soc. Geogr. It.,
686 53, 165-270.
687
688 Filella, I., Peñuelas, J. 2003. Partitioning of water and nitrogen in co-occurring Mediterranean
689 woody shrub species of different evolutionary history. Oecologia, 137, 51–61.
690
691 Giaccio, B., Regattieri, E., Zanchetta, G., Nomade, S., Renne, P.R., Sprain, C.J., Drysdale, R.N.,
692 Tzedakis, P.C., Messina, P., Scardia, G., Sposato, A., Bassinot, F. 2015. Duration and dynamics of
693 the best orbital analogue to the present interglacial. Geology, 43, 603–606.
694
695 Gioncada A., Leoni L., Lezzerini M., Miriello D., 2011. Relationships between mineralogical and
696 textural factors in respect to hydric dilatation of some sandstones and meta-sandstones from the
697 Northern Apennine. Italian Journal of Geoscience, 130, 394-403.
698
699 Giraudi, C., Zanchetta, G., Sulpizio, R. 2013. A Late-Pleistocene phase of saharan dust deposition
700 in the high Apennine Mountains (Italy). Alpine and Mediterranean Quaternary, 26 (2), 110-122.
701
702 Gocke, M., Pistovoytov, K., Kühn, P., Wiesemberg, G.L.B., Löscher, M., Kuzyakov, Y. 2011.
703 Carbonate rhizoliths in loess and their implications for paleoenvironmental reconstruction revealed
704 by isotopic composition: $\delta^{13}C$, ^{14}C. Chemical Geology, 283, 251-260.
705
706 Hearty, P.J., Miller, G.H., Stearns, C., Szabo, B.J. 1986. Aminostratigraphy of Quaternary
707 shorelines around the Mediterranean basin. Geological Society of America Bulletin, 97, 850–858.
708
709 INQUA Working Group 1995. Definitions used in Paleopedology, Paleopedology Glossary.
710 INQUA/ISSS Paleopedology Commission. Newsletter 11 (2), 35–37.
711

712 IUSS Working Group WRB. 2006. World reference base for soil resources 2006. 2nd edition.
713 World Soil Resources Reports No. 103. FAO, Rome.
714
715 Kerney, M.P., Cameron, R.A.D. 1999. Guide des escaragots et limaces d' Europe. Delachaux et
716 Niestlè, Paris 1-370.
717
718 Klappa, C.F. 1980. Rhizoliths in terrestrial carbonates: classification, recognition, genesis and
719 significance. Sedimentology, 27, 613-629.
720
721 Knauth, P.L., Brilli, M., Klonowsky, S. 2003. Isotope geochemistry of caliche developed on basalt.
722 Geochim. Cosmochim. Acta, 67, 185-195.
723
724 Kohn, M.J. 2010. Carbon isotope compositions of terrestrial C3 plants as indicators of
725 (paleo)ecology and (paleo)climate. PNAS, 107, 19691–19695.
726
727 Kühn, P., Aguilar, J., Miedema, R. 2010. Textural Pedofeatures and Related Horizons. In: Stoops,
728 G., Marcelino, V., Mees, F., (eds). Interpretation of Micromorphological Features of Soils and
729 Regoliths, Elsevier, pp. 217-250.
730
731 Jiamao, H., Keppens, E., Tungsheng, L., Paepe, R., Wenyng, J. 1997. Stable isotope composition of
732 the carbonate concretion in loess and climate change. Quat. Int., 37, 37–43.
733
734 Lambeck, K., Rouby, H., Purcell, A., Sun, Y., Sambridge, M. 2014. Sea level and global ice
735 volumes from the last glacial maximum to the Holocene. PNAS,111, 15296–15303.
736
737 Land L.S. 1989. The carbon and oxygen isotopic chemistry of surficial Holocene shallow marine
738 carbonate sediment and Quaternary Limestone and dolomite. In P. Fritz and J.Ch. Fontes:
739 Handbook of Environmental Isotope Geochemistry, 3, 191-217. Elsevier
740
741 Lazzarotto, A., Mazzanti, R., Nencini, C. 1990. Geologia e morfologia dei comuni di Livorno e
742 Collesalvetti. Quad. Mus. St. Nat. di Livorno, 11, suppl. 2, 1-58.
743
744 Leone, G., Leoni, L., Sartori, F. 1988. Revisione di un metodo gasometrico per la determinazione di
745 calcite e dolomite. Atti Soc. Toscana Sc. Nat. Mem. Serie A, 95, 7–20.

Lezzerini, M., Franzini, M., Di Battistini, G., Zucchi, D. 2008. The «Macigno» sandstone from Matraia and Pian di Lanzola quarries (north-western Tuscany, Italy). A comparison of physical and mechanical properties. Atti Soc. Toscana Sc. Nat. Mem. Serie A, 113, 71-79.

Limondin-Lozouet, N., Antoine, P. 2001. Paleoenvironmental changes inferred from malacofaunas in the Late Glacial and Early Holocene fluvial sequence at Conty, northern France. Boreas, 30, 148-164.

Lindbo, D.L., Stolt, M.H., Vepraskas, M.J. 2010. Redoximorphic Features. In: Stoops, G., Marcelino, V., Mees, F., (eds). Interpretation of Micromorphological Features of Soils and Regoliths, , pp 129-147. Elsevier

Longinelli, A, Selmo, E. 2003. Isotopic composition of precipitation in Italy: a first overall map. J. Hydrol., 270, 75–88.

Ložek, V. 1964. Quartärmollusken der Tschechoslowakei. Rozpravy Ústredniho Ústavu Geologickèho, 31, 1-374.

Ložek, V. 1986. Mollusca analysis. In: Berglund B.E. (ed) Handbook of Holocene Palaeoecology and Palaeohydrology, 729-740. Wiley, New York.

Ložek, V. 1990. Molluscs in loess, their paleoecological significance and role in geochronology principals and methods. Quat. Int., 7/8, 71-79.

Ložek, V. 2001. Molluscan fauna from the loess series of Bohemia and Moravia. Quat. Int., 76/77, 141-156.

Magnin, F. 1993. Competition between two land gastropods along altitudinal gradients in south-eastern France: neontological and paleontological evidences. J. Mol. Stud., 58, 445-454.

Marcolini, F., Bigazzi, G., Bonadonna, F.P., Centamore, E., Cioni, R., Zanchetta, G. 2003. Tephrochronology and tephrostratigraphy of two Pleistocene continental fossiliferous successions from Central Italy. J. Quat. Sc., 18, 545-556.

Martrat, B., Jimenez-Amat, P., Zahn, R., and Grimalt J. O., 2014. Similarities and dissimilarities between the last two deglaciations and interglaciations in the North Atlantic region. Quat. Sc. Rev., 99, 122-134.

Masi, A., Sadori, L., Baneschi, I., Siani, A.M., Zanchetta, G. 2013a. Stable isotope analysis of archaeological oak charcoal from eastern Anatolia as a marker of mid-Holocene climate change. Plant Biology, 15, 83-92.

Masi, A., Sadori, L., Zanchetta, G., Baneschi, I., Giardini, M. 2013b. Climatic interpretation of carbon isotope content of mid-Holocene archaeological charcoals from eastern Anatolia. Quat. Int., 303, 64-72.

Mauz, B. 1999. Late Pleistocene records of littoral processes at the Tyrrenean Coast (Central Italy): depositional environments and luminescence chronology. Quat. Sc. Rev., 18, 1173-1184.

Morse, J.W., Bender, M.L. 1990. Partition coefficients in calcite: examination of factors influencing the validity of experimental results and their application to natural systems. Chem. Geol., 82, 265–277.

Murphy, C.P. 1986. Thin Section Preparation of Soils and Sediments. Berkhamsted, A.B. Academic Publishers, 143 p

Nisi, M. F., Antonioli, F., Dai Prai, G., Leoni, G., Silenzi, S. 2003. Coastal deformation between the Versilia and the Garigliano plains (Italy) since the last interglacial stage. J. Quat. Sc., 18, 709-721.

Ottmann, F. 1954. Le Quaternaire dans la région de Quercianella-Rosignano (Livorno). Atti Soc. Tosc. Sc. Nat., 41, 23-45.

Pécsi, M. 1990. Loess is not just the accumulation of dust. Quat. Int., 7/8, 1-21.

Pierre, C. 1999. The oxygen and carbon isotope distribution in the Mediterranean water masses. Mar. Geol., 153, 41–55.

814 Pfenninger, M., Magnin, F. 2001. Phenotypic evolution and hidden speciation in Candidula
815 unifasciata ssp (Helicellinae, Gastropoda) inferred by 16S variation and quantitativeshell traits.
816 Mol. Ecol., 10, 2541-2554.
817
818 Pfenninger, M., Eppensteine, A., Magnin, F. 2003. Evidence for ecological speciation in the sister
819 species *Candidula unifasciata* (Poiret, 1801) and *C. rugosiuscula* (Michaoud, 1831) (Helicellinae,
820 Gastropa). Biol. J. Lin. Soc., 79, 611-628.
821
822 Puisségur, J.J. 1976. Mollusques continenteaux Quaternaries des Bourgogne. Significations
823 stratigraphiques et climatiques. Rapports avee d' autres faunas borèales de France. Mèmoires
824 Gèologiques Universitè de Dijon, 3, 1-241.
825
826 Raich, J.W., Schlesinger, W.H. 1992. The global carbon dioxide flux in soil respiration and its
827 relationship with vegetation and climate. Tellus, 44B, 81–99.
828
829 Ramrath, A., Sadori, L., & Negendank, J. F. (2000). Sediments from Lago di Mezzano, central
830 Italy: a record of Lateglacial/Holocene climatic variations and anthropogenic impact. The
831 Holocene, 10, 87-95.
832
833 Regattieri, E., Zanchetta, G., Drysdale, R.N., Isola, I., Hellstrom, J.C., Roncioni, A. 2014a. A
834 continuous stable isotopic record from the Penultimate glacial maximum to the Last Interglacial
835 (160 to 121 ka) from Tana Che Urla Cave (Apuan Alps, central Italy). Quat. Res., 82, 450–461.
836
837 Regattieri, E., Zanchetta, G., Drysdale, R.N., Isola, I., Hellstrom, J.C., Dallai, L. 2014b. Lateglacial
838 to Holocene trace element record (Ba, Mg, Sr) from Corchia Cave (Apuan Alps, central Italy):
839 paleoenvironmental implications. J. Quat. Sc., 29, 381–392.
840

841 Regattieri, E., Giaccio, B., Galli, P., Nomade, S., Peronace, E., Messina P., Sposato, A., Boschi, C.,
842 Gemelli, M. 2016. A multi-proxy record of MIS 11-12 deglaciation and glacial MIS 12 instability
843 from the Sulmona Basin (central Italy). Quat. Sc. Rev., 32, 129-145.

844

845 Regattieri, E., Giaccio, B., Zanchetta, G., Drysdale, R. N., Galli, P., Nomade, S., Peronace, E.,
846 Wulf, S. 2015. Hydrological variability over the Apennines during the Early Last Glacial precession

847 minimum, as revealed by a stable isotope record from Sulmona basin, Central Italy. J. Quat. Sc., 30,
848 19-31.
849
850 Reimer, P. J., Bard, E., Bayliss, A., Beck, J.W., Blackwell, P.G., Bronk Ramsey, C., Buck, C.E.,
851 Cheng, H., Edwards, R.L., Friedrich, M., Grootes, P.M., Guilderson, T.P., Haflidason, H., Hajdas,
852 I., Hatté, C., Heaton, T.J., Hoffmann, D.L., Hogg, A.G., Hughen, K.A., Kaiser, K.F., Kromer, B.,
853 Manning, S.W., Niu, M., Reimer, R.W., Richards, D.A., Scott, E.M., Southon, J.R., Staff, R.A.,
854 Turney, C.S.M., van der Plicht, J. 2013. INTCAL13 and MARINE13 radiocarbon age calibration
855 curves 0-50,000 years cal BP. Radiocarbon, 55, 1869-1887.
856
857 Retallack, G.J. 1990. Soils of the Past: An Introduction to Paleopedology. Unwin Hyman, London,
858 p. 520.
859
860 Retallack, G.J. 2005. Pedogenic carbonate proxies for amount and seasonality of precipitation in
861 paleosols. Geology, 33, 333-336.
862
863 Roberts, N., Jones, M.D., Benkaddur, A., Eastwood, W.J., Filippi, M.L., Frogley, M.R., Lamb,
864 H.F., Leng, M.J., Reed, J.M., Stein, M., Stevens, L., Valero- Garcè, B., Zanchetta, G. 2008 Stable
865 isotope records of Late Quaternary climate and hydrology from Mediterranean lakes: the ISOMED
866 synthesis. Quat. Sc. Rev., 27, 2426-2441.
867
868 Rohling, E.J., Foster, G.L., Grant, K.M., Marino, G., Roberts, A.P., Tamisiea, M.E., Williams, F.
869 2014. Sea-level and deep-sea-temperature variability over the past 5.3 million years. Nature, 508,
870 477-482.
871
872 Sanesi, G. 1977. Guida alla descrizione del suolo. C.N.R., Firenze, p. 157.
873
874 Sarti, G., Zanchetta, G., Ciulli, L., Colonese, A. 2005. Late Quaternary oligotypical non-marine
875 mollusc fauna from southern Tuscany: climatic and stratigraphic implications. GeoActa, 4, 159-
876 167.
877
878 Shakun, J.D., Lea, D.W., Lisiecki, L.E., Raymo, M.E. 2015. An 800-kyr record of global surface
879 ocean $\delta^{18}O$ and implications for ice volume-temperature coupling. E. Planet. Sc. Let., 426, 58–68.
880

881 Sparks, B.W. 1961. The ecological interpretation of Quaternary non-marine Mollusca. Proc. Linn.
882 Soc. Lond., 172, 71-80.
883
884 Stoops, G. 2003. Guidelines for Analysis and Description of Soil and Regolith Thin Sections. Soil
885 Science Society of America, Madison, WI, p. 184.
886
887 Stoops, G. 2007. Micromorphology of soils derived from volcanic ash in Europe: a review and
888 synthesis. European Journal of Soil Science, 58, 356–377.
889
890 Stoops, G., Marcelino, V., Mees, F., 2010. Interpretation of Micromorphological Features of Soils
891 and Regoliths. Elsevier, p. 752.
892
893 Velentini, R., Scarasci Mugnozza, G.E., Ehleringer, J.R. 1992. Hydrogen and carbon isotope ratios
894 of selected species of a Mediterranean macchia ecosystem. Func. Ecol., 6, 627-631.
895
896 Wang, Y, Zheng, S. 1989. Paleosol nodules as Pleistocene paleoclimatic indicators, Louchuan, P.R.
897 China. Palaeogeogr., Palaeoclimatol., Palaeoecol., 76, 39–44.
898
899 White, A.F., Bullen, T.D., Vivit, D.V., Schulz, M.S., Clow, D.W. 1999. The role of disseminated
900 calcite in the chemical weathering of granitoid rocks. Geochim. Cosmochim. Acta, 63, 1939–1953.
901
902 Zanchetta, G., Bonadonna, F.P., Leone, G. 1999. A 37-meter record of paleoclimatological events
903 from stable isotope data on molluscs in Valle di Castiglione, near Rome, Italy. Quat. Res., 52, 293-
904 299.
905
906 Zanchetta, G., Bonadonna, F.P., Marcolini, F., Ciampalini, A., Fallick, A.E., Leone G., Michelucci,
907 L. 2004. Intra-Tyrrhenian cooling event deduced by non-marine mollusc assemblage at Villa S.
908 Giorgio (Livorno, Italy). Boll. Soc. Paleont. It., 43, 331-343.
909
910 Zanchetta G., Leone G., Fallick A.E., Bonadonna F.P. 2005. Oxygen isotope composition of living
911 land snail shells: data from Italy. Palaeogeogr., Palaeoclimatol., Palaeoecol., 223, 20-33.
912
913 Zanchetta, G., Becattini, R., Bonadonna, F.P., Bossio, A., Ciampalini, A., Colonese, A.,
914 Dall'Antonia B., Fallick, A.E., Leone, G., Marcolini, F., Mariotti Lippi, M., Michelucci, L. 2006.

915 Late Middle Pleistocene cool non-marine mollusc and small faunas from Livorno (Italy). Riv. It.
916 Paleont. Strat., 112, 135-155.
917
918 Zanchetta, G., Borghini, A., Fallick, A.E., Bonadonna, F.P., Leone, G. 2007a. Late Quaternary
919 palaeohydrology of Lake Pergusa (Sicily, southern Italy) as inferred by stable isotopes of lacustrine
920 carbonates. J. Paleolimnol., 38, 227-239.
921
922 Zanchetta, G., Drysdale, R.N., Hellstrom, J.C., Fallick, A.E., Isola, I., Gagan, M., Pareschi, M.T.
923 2007b. Enhanced rainfall in the western Mediterranean during deposition of Sapropel S1: stalagmite
924 evidence from Corchia Cave (Central Italy). Quat. Sc. Rev., 26, 279-286.
925
926 Zanchetta, G., Di Vito, A., Fallick, A.E., Sulpizio, R. 2000. Stable isotopes of pedogenic
927 carbonate from Somma-Vesuvius area, Southern Italy, over the last 18 ka: palaeoclimatic
928 implications. J. Quat. Sc., 15, 813-824.
929
930 Zanchetta, G., Bar-Matthews, M., Drysdale, R.N., Lionello, P., Ayalon, A., Hellstrom, J.C., Isola,
931 I., Regattieri, E. 2014. Coeval dry events in the central and eastern Mediterranean basin at 5.2 and
932 5.6 ka recorded in Corchia (Italy) and Soreq Cave (Israel) speleothems. Glob. Planet.Ch.,122, 130-
933 139.
934
935 Zanchetta' G., Regattieri' E., Isola, I., Drysdale, R.N, Bini, M., Baneschi, I., Hellstrom, J.C.. 2016.
936 The so-called "4.2 event" in the central Mediterranean and its climatic teleconnections. Alpine and
937 Mediterranean Quaternary, 29, 2016, 5 – 17.
938
939 Zerboni, A., Trombino, L., Cremaschi, M. 2011. Micromorphological approach to polycyclic
940 pedogenesis on the Messak Settafet plateau (central Sahara): formative processes and
941 palaeoenvironmental significance. Geomorphology, 125, 319-335.
942

943
944
945 Figure and table captions
946
947
948 Figure 1. Location Map
949
950 Figure 2. Stratigraphy of the Buca dei Corvi section (after Ciulli, 2005). Ages are reported as ka.
951 See text for detailed description.
952
953 Figure 3. Upper section of Buca dei Corvi section. (A) Panoramic view of the top of the Buca dei
954 Corvi–section, and the relationship between the lithostratigraphic units and the major bounding
955 surfaces. (B) Measured sedimentological log (modified from Ciulli, 2007). See Figure 1 for
956 location.
957
958 Figure 4 (A) $\delta^{18}O$ vs $\delta^{13}C$ of pedogenic carbonate from Buca dei Corvi section and modern
959 pedogenic carbonate from coastal Tuscany. For LU8 and LU9 hypocoatings and nodules are
960 reported separately; (B) Concretion from modern soil; (C) Hypocoatings from LU9. Black bars in
961 (B) and (C) correspond to 1 cm.
962
963 Figure 5. LU9 weathering profile, horizon BCk, thin section. (A) Channel microstructure associated
964 to a high porosity; orthic nodules (red arrows) and mollusc fragment (black arrow); Ch=chamber;
965 Cl=channel–PPL. (B) Close to single spaced porphyric c/f related distribution with dominant coarse
966 quartz grains embedded in a yellowish brown to brown micromass; strongly impregnated typic
967 nodule (white arrow)–PPL. (C) Ferruginous internal hypocoating on a shell fragment and dark
968 brown Fe-Mn segregations into the matrix; isolated reddish fragment of clay coating incorporated in
969 the groundmass (red arrow)–PPL. (D) Different generations of fragmented clay coatings
970 incorporated in the groundmass: pure clay coatings are yellow (black arrows) while dusty clay
971 coatings are reddish (red arrow)–PPL. (E) Unweathered quartz grains, rock fragments and poorly
972 weathered primary mineral grains dominate the coarse particle size fraction; dense incomplete
973 calcite infillings locally impregnated by brownish ferruginous segregations–XPL. (F) Complex c/f
974 related distribution: close to single spaced porphyric, locally chito–gefuric; strongly impregnated,
975 typic anorthic nodule (white arrow) and shell fragment (red arrow)–XPL. (G) Loose discontinuous
976 calcite crystalline pedofeatures within a large channel; crystallitic b-fabric is common in

977 correspondence with large concentrations of calcite in the fine fraction–XPL. (H) Fe-Mn
978 impregnations on dense incomplete calcite infillings, up to 4 mm thick; fragment of reddish dusty
979 clay coatings (white arrow)–XPL.
980
981 Figure 6. Geochemical and isotopic data from Buca dei Corvi section
982
983 Figure 7. Comparison between chemical composition of Macigno Formation and LU8 and LU9
984 deposits from Buca dei Corvi section. Macigno data from Lezzerini et al. (2008) and Gioncada et al.
985 (2011).
986
987 Figure 8. From the top to the bottom: Relative sea level (Lambeck et al., 2014); $\delta^{18}O$ of stalagmite
988 CC26 from Corchia Cave (Zanchetta et al., 2007b); $\delta^{18}O$ from NGRIP ice core (NGRIP members,
989 2004); Monticchio pollen data (Brauer et al., 2007); SST from core ODP 976 (Martrat et al., 2014).
990 Radiocarbon dating, this work; OSL dating from Mauz (1999); chronology of the end of deposition
991 of loess in Apennine (Giraudi et al., 2013).
992
993 Table 1. Stable isotope results from hypocoatings (°) and nodules (*) from Aurelia section (LU9
994 and LU8). Note that there are not systematic differences between the different kinds of carbonate
995 concretions.
996
997 Table 2. Stable isotope composition of modern rhizoconcretions collected at Baratti and
998 Castiglioncello (see Fig. 1). Concretions were collected along living roots in the modern soils.
999
1000 Table 3. Radiocarbon dating of concretions along LU8 and LU9. Calibration was performed using
1001 INTCAL13 database (Reimer et al., 2013).
1002
1003 Table 4. Via Aurelia section non-marine mollusc species grouped by ecological classes; number of
1004 specimens and their percentages are indicated. Ecological classes: 4 - steppe species; 5 - open land
1005 species.

Highlights

A multiproxy environment reconstruction from Late Glacial deposit of Central Italy is proposed;

Pedogenic features, land snail association and stable isotopes indicate dry climate condition;

$\delta^{18}O$ values of pedogenic carbonates indicates that $\delta^{18}O$ of precipitation was higher than present.

Table

Click here to download Table: Boretto_Table_1.docx

Sample	Depth (m a.s.l.)[1]	$\delta^{13}C$ ‰ (V-PDB)	$\delta^{18}O$ ‰ (V-PDB)
BCA10/1°	28.30	-8.93	-3.88
BCA10/2°	"	-8.60	-3.96
BCA10/3*	"	-8.27	-3.82
BCA9/1°	28.00	-8.39	-3.52
BCA9/2°	"	-8.68	-3.40
BCA9/3*	"	-7.34	-3.21
BCA8/1°	27.7	-6.52	-2.85
BCA8/2°	"	-5.82	-2.51
BCA8/3°	"	-6.52	-2.77
BCA7/1°	27.4	-6.51	-2.99
BCA7/2°	"	-6.69	-2.95
BCA7/3*	"	-6.26	-2.75
BCA6/1°	27,10	-6.65	-3.04
BCA6/2°	"	-6.52	-3.15
BCA6/3*	"	-6.00	-2.75
BCA5/1°	26.90	-6.92	-3.46
BCA5/2°	"	-7.17	-3.16
BCA5/3*	"	-6.87	-3.46
BCA4/1°	26.60	-7.62	-3.74
BCA4/2°	"	-8.54	-4.03
BCA4/3*	"	-8.55	-4.78
BCA3/1°	26.30	-8.61	-4.41
BCA3/2°	"	-8.85	-4.02
BCA3/3*	"	-8.96	-4.70
BCA2/1°	25.25	-8.75	-3.76
BCA2/2°	"	-8.09	-3.94
BCA2/3*	"	-7.41	-3.43

°Carbonate hypocoatings
*Carbonate nodules
See figure 4 for the position of the sampled section

Table

Click here to download Table: Boretto_Table_2.docx

Locality/Label	$\delta^{13}C$ ‰ (V-PDB)	$\delta^{18}O$ ‰ (V-PDB)
Castiglioncello		
Cast-1	-10.48	-4.17
Cast-2	-10.53	-4.02
Cast-3	-10.49	-4.08
Cast-4	-10.48	-3.74
Cast-5	-10.59	-3.97
Baratti		
Bar16	-10.07	-4.76
Bar15	-10.05	-4.69
Bar10	-10.39	-4.82
Bar9	-10.35	-4.52
Bar8	-10.31	-4.57
Bar7	-10.5	-4.47
Bar6	-9.90	-4.62
Bar5	-9.53	-4.89
Bar3	-9.77	-4.73

Table

Click here to download Table: Boretto_Table_3.docx

Sample	Laboratory code	Conventional Radiocarbon Age (yr BP)	Calibrated Radiocarbon Age (±2σ) (Median probability)	$\delta^{13}C$ (‰ V-PDB)
BCA D.6 (28.2 m a.s.l.)*	Beta-235367	9980±50	11253 – 11629 (11440)	-7.6
BCA.D.4 (27.7 m a.s.l.)*	Beta-235368	11310±50	13074 – 13268 (13161)	-5.3

Table

Click here to download Table: Boretto_Table_4.docx

Ecological Group	Species	Number of specimens	Percentage (%)
4	*Candidula unifascita*	1224	79
4	*Jamina quadridens*	17	1
Sub-total		*1241*	*80*
5	*Pupilla moscorum*	182	12
5	*Vallonia pulchella*	126	8
Sub-total		*308*	*20*
Total		**1549**	**100**

Figure

Click here to download high resolution image

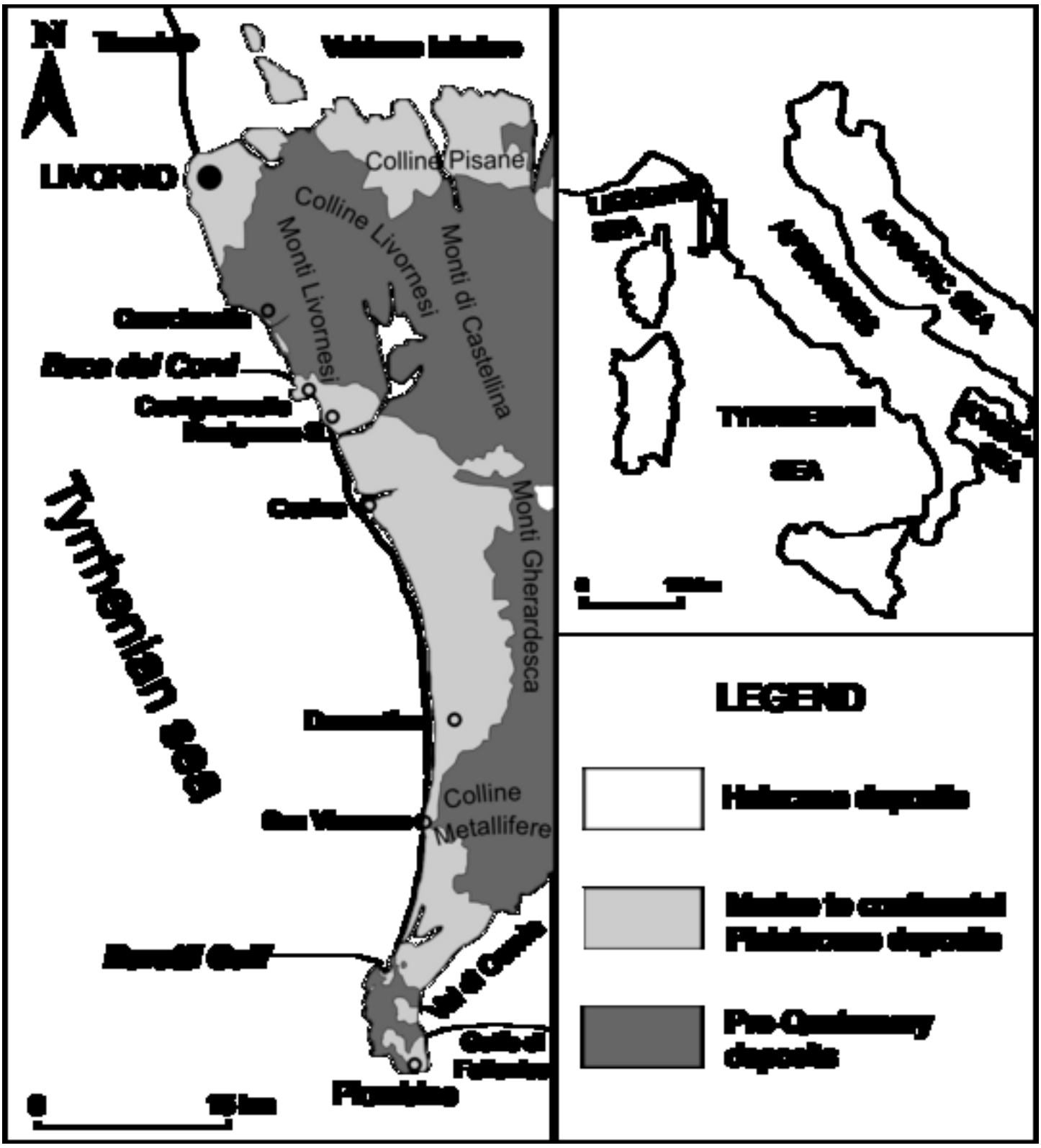

Figure
Click here to download high resolution image

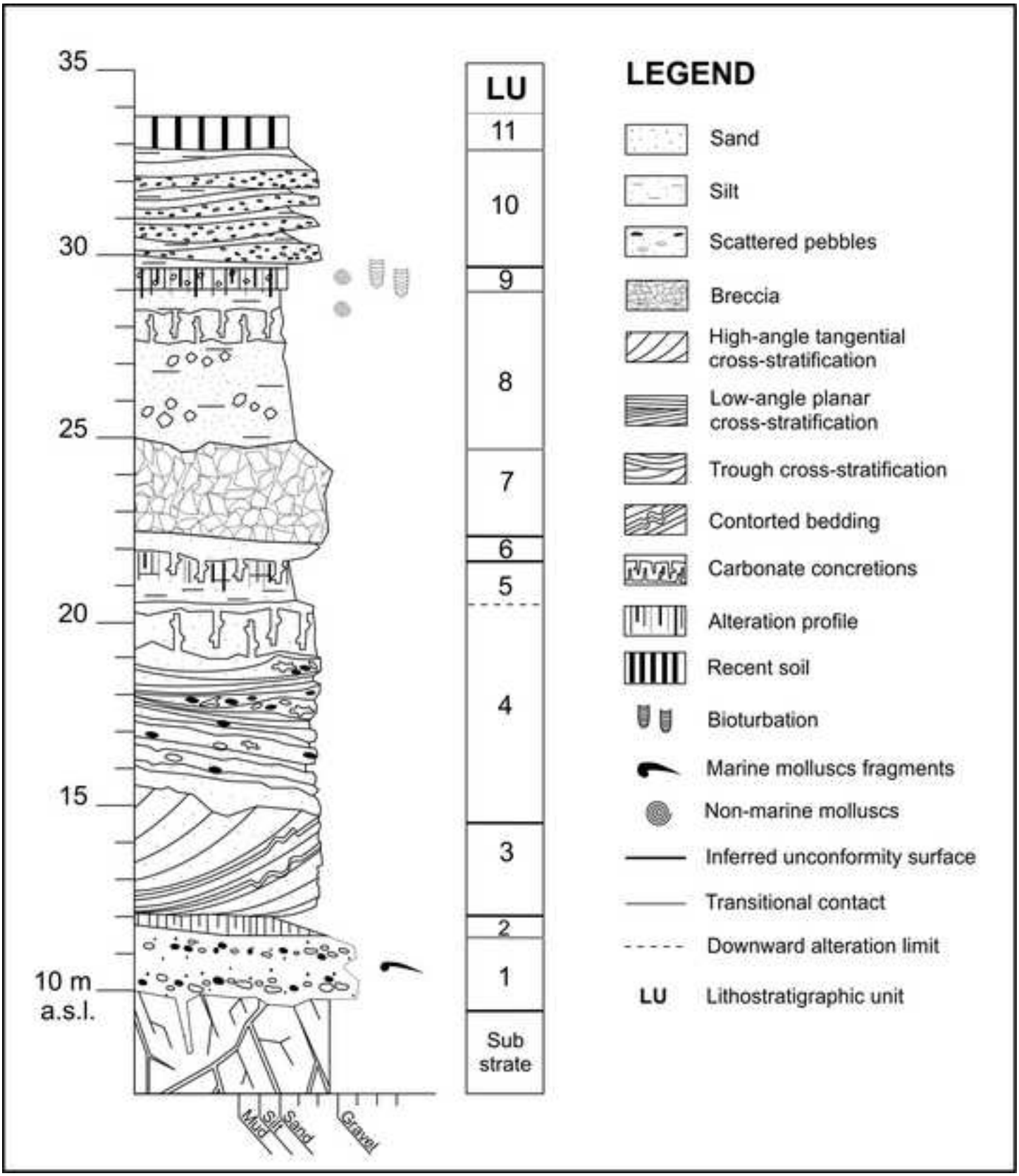

Figure
Click here to download high resolution image

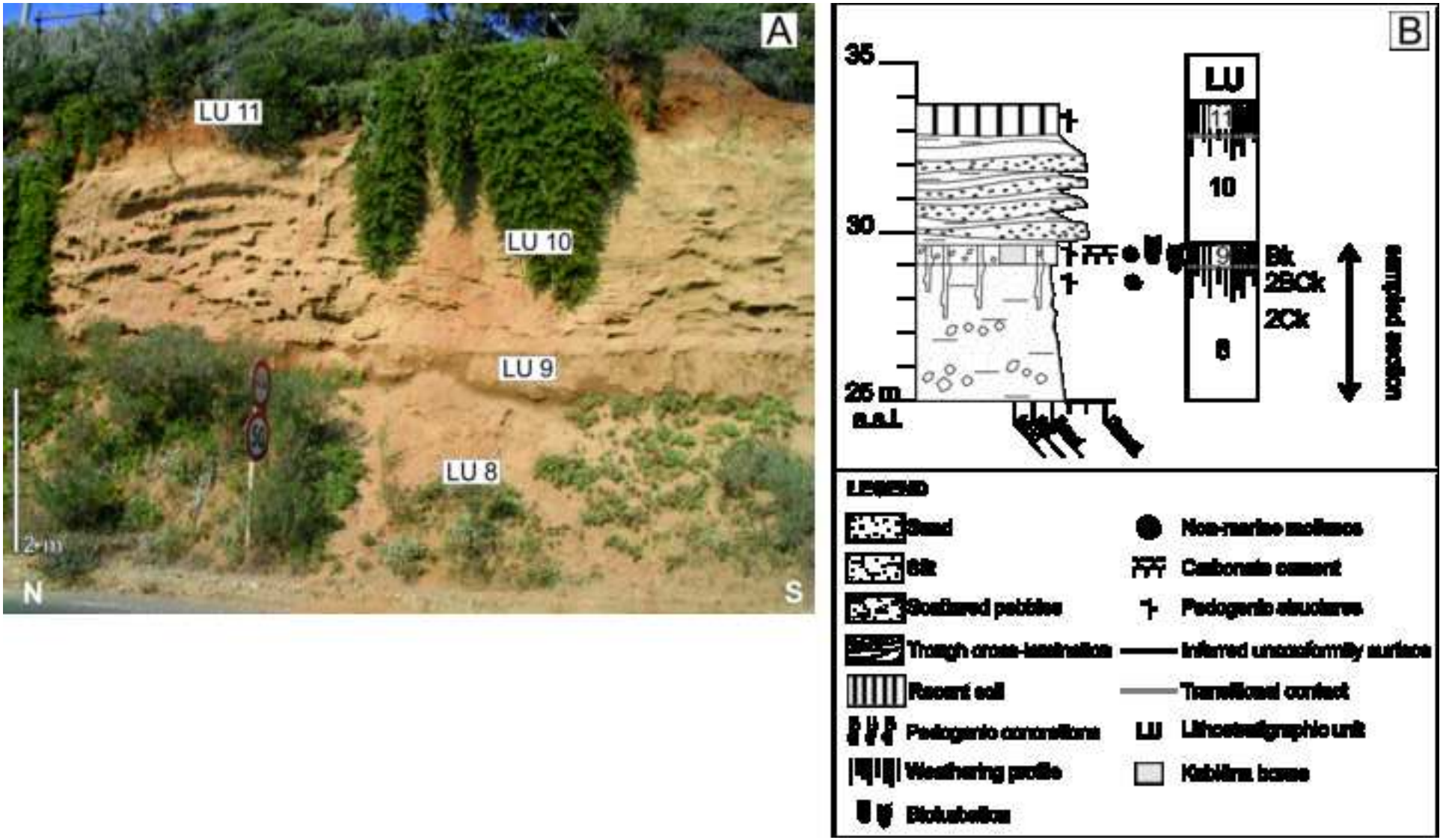

Figure
Click here to download high resolution image

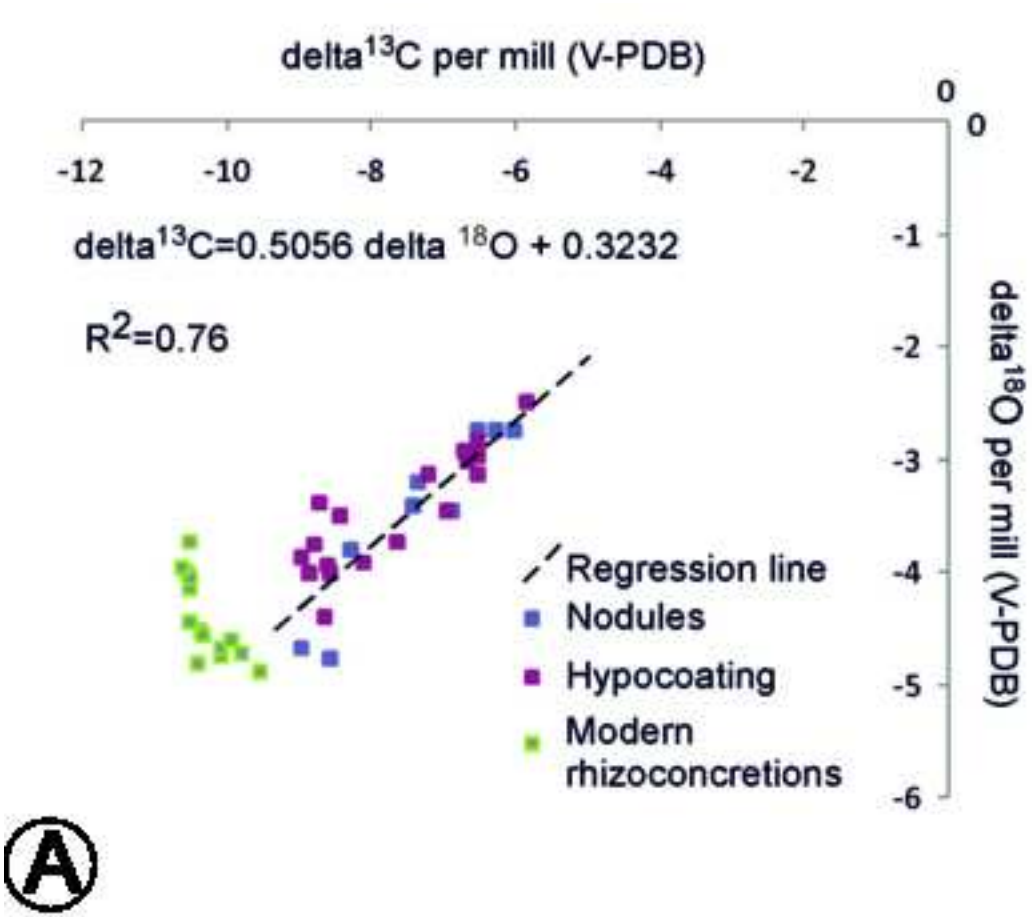

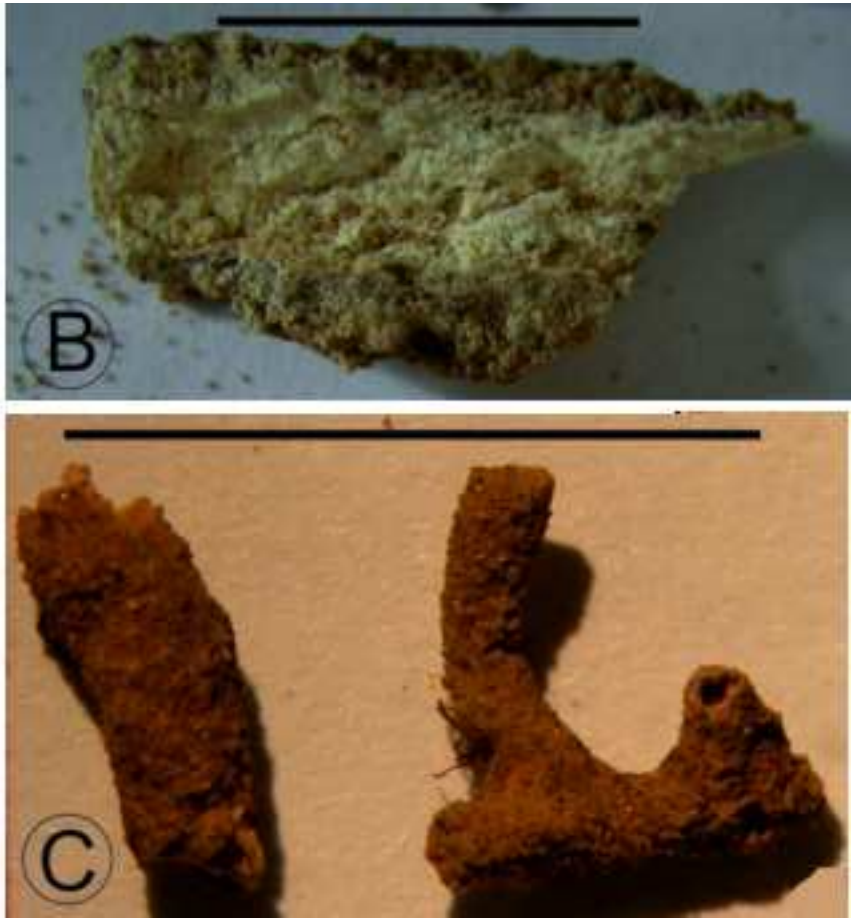

Figure

Click here to download high resolution image

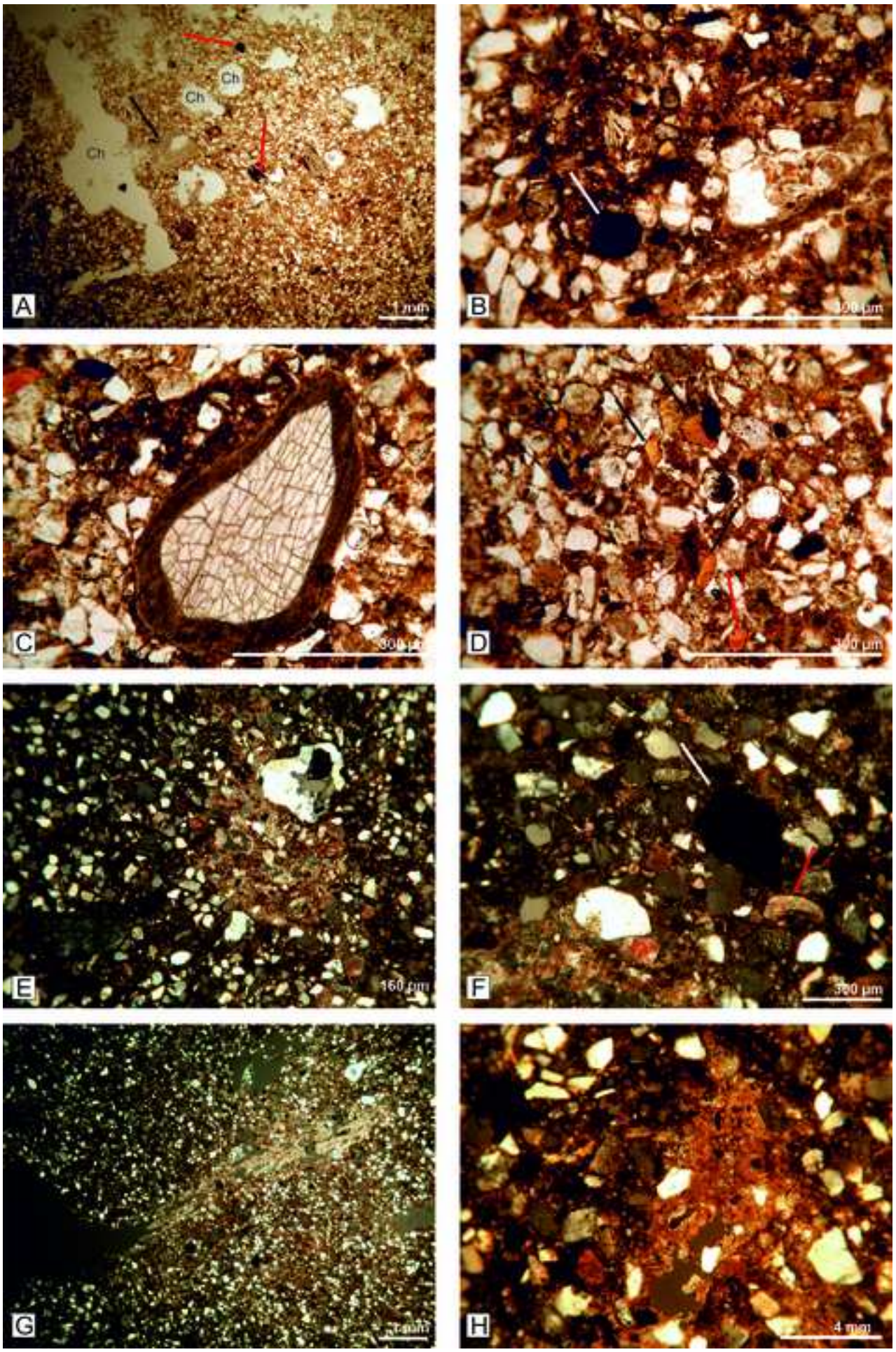

Figure
Click here to download high resolution image

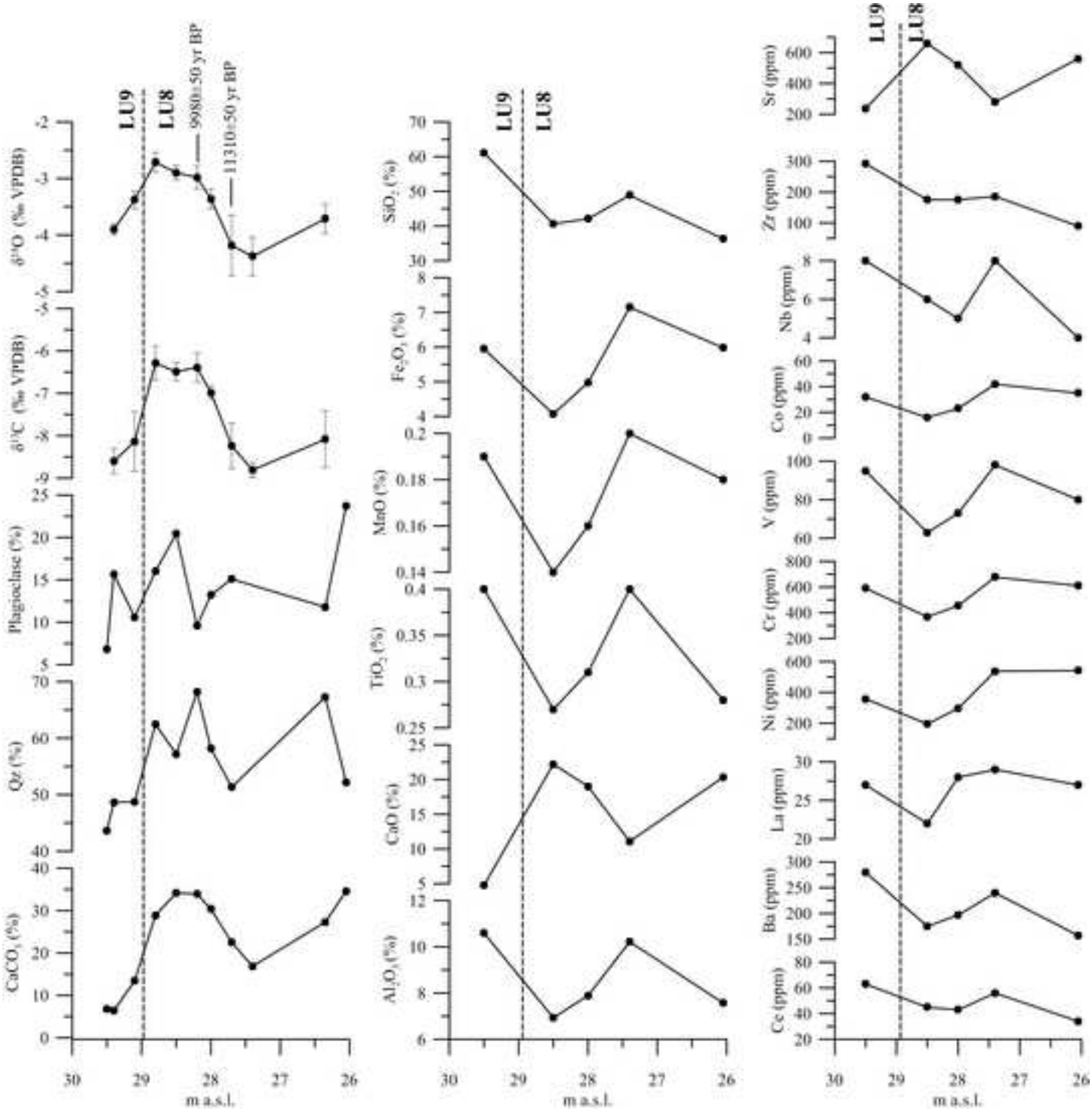

Figure
Click here to download high resolution image

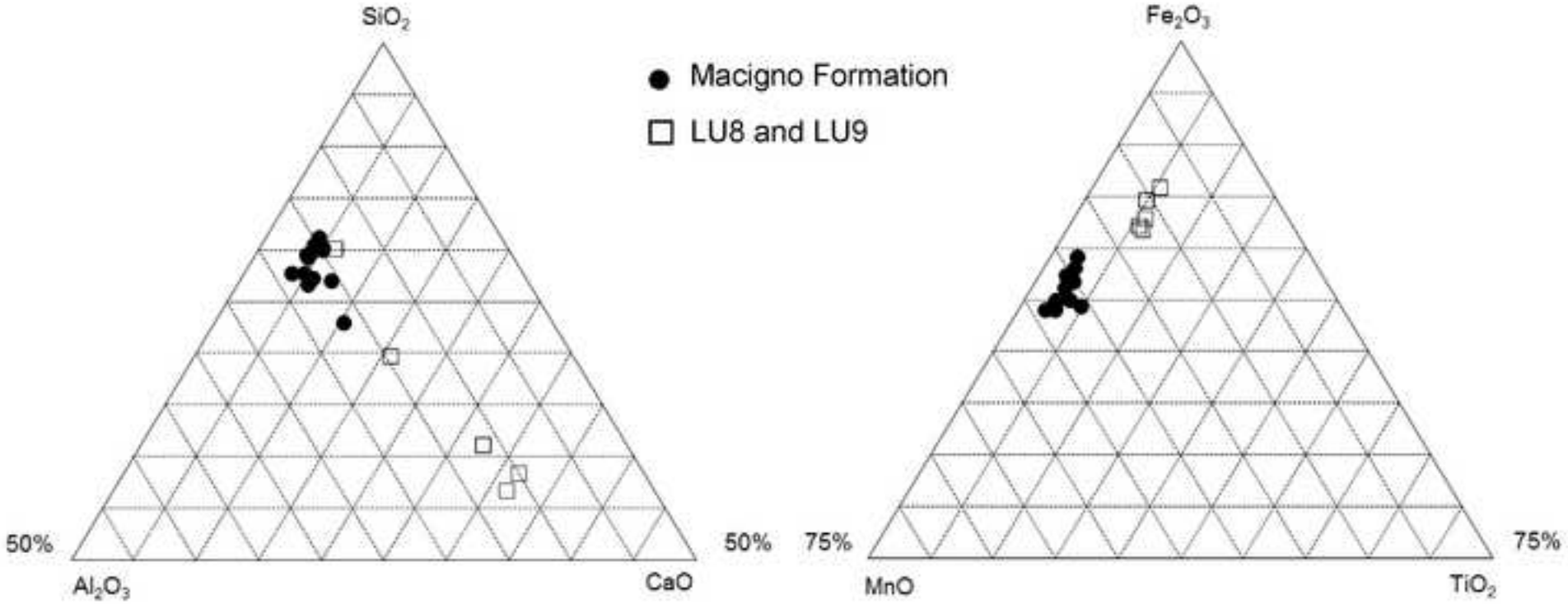

Figure

Click here to download high resolution image